EE-7 | 1345

MILITARY TECHNICAL COLLEGE

CAIRO - EGYPT

DESIGN OPTIMIZATION OF RELUCTANCE MOTORS USING A FIELD APPROACH

Mostafa El-Shebiny*

ABSTRACT

In order to improve performance of reluctance motors, careful design of the magnetic circuit is necessary. The machine reluctance is a determining parameter in the design process.

In this paper several techniques for designing the magnetic circuit are proposed. A fields approach is applied and computer programs are used for numarical solutions. The proposed techniques lead to optimised values of the ratio between (K_{ad}) and(K_{aq}) e.g. the anistropy coefficient. Theoritical prediction for the performance of a designed model is performed and computed results are reported.

* Department of Electrical Power and Machines Engineering, Faculty of Engineering and Technology, Menoufia University, Shebin El-Kom, Egypt.

I. INTRODUCTION

The reluctance motor is a robust machine but not so complex, that resembles the squirrel cage induction motor. Due to its nice properties such as synchronous operation, absence of sparks, low noise, etc., it has been used in some applications. Namely, the driving of inertia generators for computer power supplies, fans and it can be used also in systems of explosive media.

The above mentioned advantages make this reluctance motor competative, from the technical and economic points of view, with the ordinary synchronous motor.

In the reluctance motor, the higher the magnetic isotropy of the magnetic rotor circuit, the higher the pullout torque, the efficiency and the power factor.

In this paper, the isotropy coefficient of the machine defined by the ratio between (K_{ad}) and (K_{aq}) ($K = K_{ad}/K_{aq}$) is calculated. where K_{ad} and K_{aq} are the form factors of magnetic field in the air-gap.

The magnetic field of the reluctance motor will be calculated as a function of rotor geometries and air-gap parameters[1].

The highest values of the magnetic anisotropy [K] will occur at the flux barrier of the reluctance rotor; a detailed study of such a problem will be included in this paper later.

2. MATHEMATICAL MODEL

The equation of magnetic field can be deduced by integrating the Laplace equation for the scalar magnetic potential under the following conditions:

a] Unsaturated magnetic circuit, which allow separate computations along direct and quadrature axes.

b] The distribution of the scalar magnetic potential produced by the stator winding, at the margin of the stator, is assumed to be sinusoidal;

c] The machine is also assumed to be of infinite length. according to the rotor symmetry, computations were carried out only for a sector corresponding to a pole pitch.

2.1. Flux Distribution Computation for Quadrature Axis

Fig. 1 shows the flux distribution for q-axis. Using the notation of Fig. 1, the magnetizing force distribution for the non-magnetic region is

$$\text{for sector I} \quad H_{cn1} = [U_o/(\theta_{cn}.R_5)] \qquad (1)$$

$$\text{for sector II} \quad H_{cn2} = [U_o/(R_2-R_1)]$$

The magnetizing force distribution for area ABCDEFGHIJKLA , is found by integrating the Laplace equation of the scaler magnetic potential U, in polar coordinates.

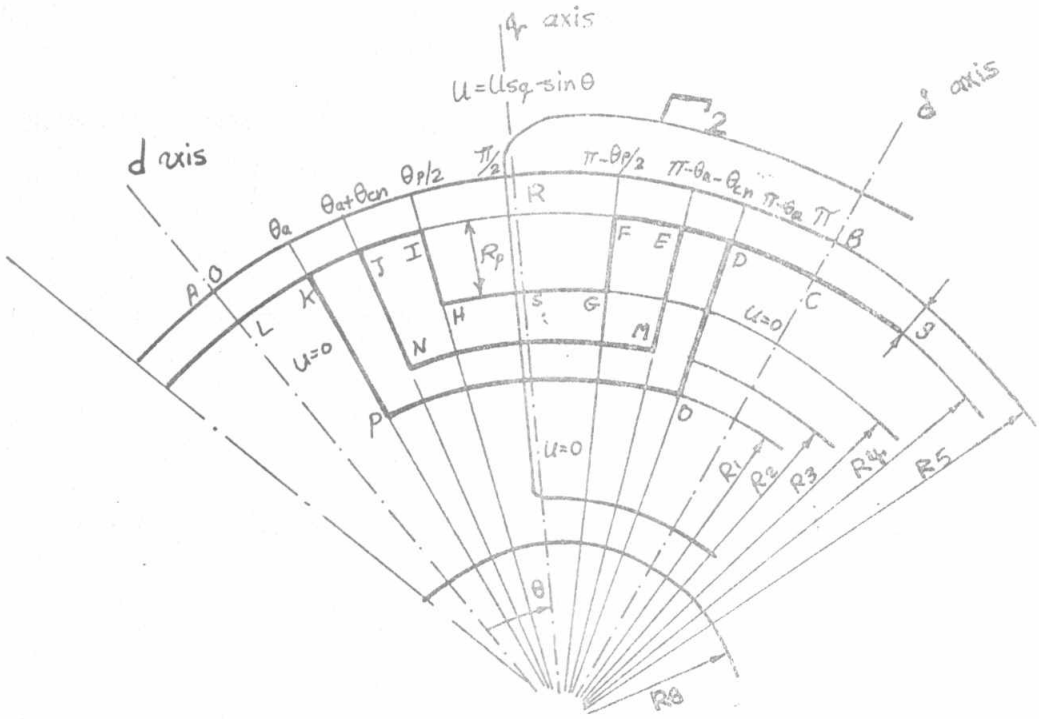

Fig.(1) Flux distribution for quadrature axis

$$\frac{\partial^2 u}{\partial r^2} + \frac{1}{r}\frac{\partial u}{\partial r} + \frac{1}{r^2}\frac{\partial^2 u}{\partial \theta^2} = \theta \qquad (2)$$

with the following boundary conditions:

$$\begin{aligned}
&U|AB=U(R_5,\theta)=U_{sq}\sin\theta; && 0\leq\theta\leq\pi\ ;\\
&U|CD=U(KL)=U(R_4,\theta)=0\ ; && 0\leq\theta\leq\theta_a \text{ and } (\pi-\theta_a)\leq\theta\leq\pi\ ;\\
&U|EF=U|IJ=U(R_4,\theta)=U_o; && (\theta_a+\theta_{cn})\leq\theta\leq\theta p/2 \text{ and } (\pi-\theta p/2)\leq\theta\leq\pi-\theta_a-\theta_{cn}; \qquad (3)\\
&U|GH=U(R_3,\theta)=U_o\ ; && \theta p/2\leq\theta\leq(\pi-\theta p/2)\\
&U|FG=U(r,\pi,\theta p/2)=U_o; && R_3\leq r\leq R_4
\end{aligned}$$

Due to the continuity of $U(r,\theta)$, along BC and AL, then :

$$\begin{aligned}
&U|BC=U(r,\pi)=\theta; && R_4\leq r\leq R_5\ ;\\
&U|LA=U(r,0)=0 && R_4\leq r\leq R_5
\end{aligned} \qquad (4)$$

Taking the linear variation of U into consideration, the magnetic potentials along DE and JK are :

$$U|ED=U(R_4,\theta)=U_o-\frac{U_o}{\theta_{cn}}[\theta-(\pi-\theta_a-\theta_{cn})]\ ,$$

for $(\pi-\theta_a-\theta_{cn})\leq\theta\leq(\pi-\theta_a)$ (5)

$$U|KJ=U(R_4,\theta)=\frac{U_o}{\theta_{cn}}[\theta-\theta_a]$$

Because RS is part of a flux line Γq, then :

$$\begin{aligned}
F_{sq} &= F_q + F_o\\
F_q &= F\sin\delta\\
F &= \frac{B_g}{\mu o}.g
\end{aligned} \qquad (6)$$

where B_g is the maximum air-gap flux density, δ is the motor load angle, $g = R_5 - R_4$ is the minimum machine air-gap, and F_q is the air-gap magnetizing force on q-axis.

In order to determine F_o for a machine whose length is ℓ, the magnetic flux low is applied for the surface supported by the curve EFGHIGNME, for which the flux value is :

$$\phi_1 = \phi|_{JNME} = (2.JN.\frac{F_o}{\theta_{cn}.R_5} + MN.\frac{F_o}{R_2-R_1})\ \mu o.\ell \tag{7}$$

which has to be equal to the flux

$$\phi_2 = \phi|_{EFGHIJ} = [|(H_r|_{EF})|\ .EF + |(H_\theta|_{FG}|.\ FG + |(H_r|_{GH}).GH - |(H\theta|_{HI})|.HI + (|H_r|_{IJ}).\ IJ]\ \mu o.\ \ell \tag{8}$$

where

$$H_r = \frac{-\partial F(r,\theta)}{\partial r}\ ;\quad H_\theta = -\frac{1}{r}\ \frac{\partial F(r,\theta)}{\partial \theta} \tag{9}$$

are the radial and tangential components of the magnetizing force. By taking into account the fact that ϕ_1 and ϕ_2 are a linear functions of F_o, it is sufficient to take two arbitrarily chosen values of F_o (e.g. F_{o1}, F_{o2})

$$\phi_{11} = \phi_1|F_o = F_{o1}\ ;\ \phi_{21} = \phi_2|F_o = F_{o1}$$
$$\phi_{22} = \phi_2|F_o = F_{o2}\ ;\ \theta_{12} = \theta_1|F_o = F_{o2} \tag{10}$$

and the value of F_o, for q-axis is found at the intersection of

$$\phi_1 = F_1(F_o) \text{ and } \phi_2 = f_2(F_o)\ ;$$

$$F_{oq} = \frac{(\phi_{21} - \phi_{11})(F_{o2} - F_{o1})}{(\phi_{12} - \phi_{11})-(\phi_{22} - \phi_{21})} + F_{o1}\ . \tag{11}$$

Using this value, the air-gap magnetizing force distribution can be calculated as follows :

$$H_{g_{qr}} = \frac{\partial F(r,\theta)}{\partial r}\Big|_{r=R_5}\ ,\quad H_{g_{q\theta}} = -\frac{1}{R_5}\ \frac{\partial F(r,\theta)}{\partial \theta}\Big|_{r=R_5} \tag{12}$$

the air-gap flux densities are :

$$B_{g_{qr}} = \mu_o H_{g_{qr}}\ ;\quad B_{g_{q\theta}} = \mu_o H_{g_{q\theta}} \tag{13}$$

By integrating the Laplace equation, the magnetic flux density is determined. Fig. 2 illustrates the air-gap flux density in q-axis.

It is noticed that the first significant decrease of the flux density occurs for an angle $_a$ from the pole axis. A reversal of the flux density pole can be even take place if the scalar magnetic potential U_o is larger than the value corresponding to the sinusoidal of the scalar magnetic potential at that particular point

$$U_o > U_{sq} \sin(\theta_a + \theta_{nc})$$

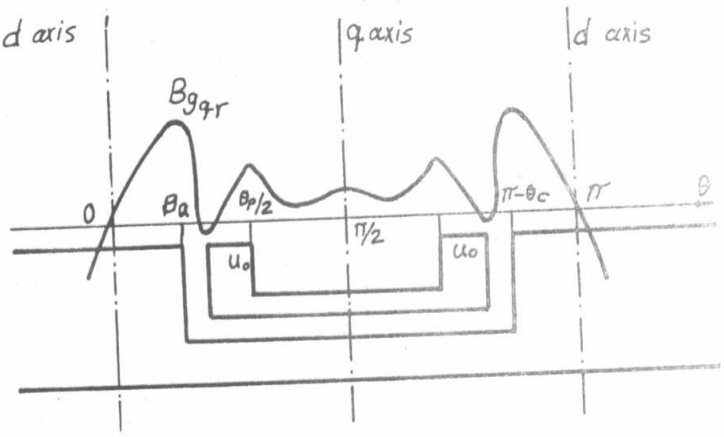

ig.(2) Air-gap magnetic field flux distribution for q-axis

A second decrease of the flux density occurs due to the increased air-gap between the poles.

The amplitude of the flux density fundamental is found by expanding into fourier series;

$$B_{g_{q1}} = \frac{4}{\pi} \int_{o}^{\pi/2} b_{g_{qr}}(\theta) \sin\theta \, d\theta \qquad (14)$$

For an isotropic equivalent cylindrical rotor, the maximum flux density on q-axis is found by

$$B_{g_{qc}} = B_g \sin\delta$$

The form factor K_{aq} is defined as the ratio of the fundamental harmonic amplitude of the air-gap flux density of the real machine, to the fundamental hormonic amplitude for an ideal cylindrical one

$$K_{aq} = \frac{B_{g_{q1}}}{B_{g_{qc}}} \qquad (15)$$

Other coefficients necessary for the motor design are :

i] The pole pitch covering coefficient α_q is the pole pitch covering coefficient of an ideal machine which has the same flux as the real machine, whose flux distribution is constant and equal to the maximum flux distribution on q-axis, $B_{g_{qm}}$.

$$\alpha_q = \frac{\phi_q}{\tau . \ell . B_{q_{rm}}} \quad , \quad \text{where} \quad \tau = \pi . R_5$$

$$\phi_q = \int_{o}^{\pi} b_{g_{qr}}(\theta) \, R_5 . \ell . d\theta \qquad (16)$$

ii] The form coefficient of the flux for q-axis ($K\phi_q$)

$$K\phi_q = \frac{\phi_q}{\phi_{q1}} ,$$

where

$$\phi_{q1} = \int_{o}^{\pi} B_{g_{q1}} \sin\theta \, R_5 \, \ell . d\theta \qquad (17)$$

is air-gap fundamental flux distribution on q-axis.

2.2. Calculation of the Flux Distribution on d-axis

The following modifications occur

$$F|_{AB} = F(R_5,\theta) = F_{sd}\cos\theta \quad 0\leq\theta\leq\pi \quad , \tag{18}$$

$$F|_{BC} = F(r,\pi) = -\frac{r - R_4}{R_5 - R_4} F_{sd} \quad R_4\leq r\leq R_s ,$$

$$F|_{LA} = -F|_{BC}$$

the remaining boundary conditions are the same as for the computation for q-axis. As in q-axis, the scalar magnetic potential along AB is cosinusoidal, the flux coming out of EFGS is equal to the one entering SHIJ and hence, the overall flux for EFGHIJ is zero; $\phi_2 = 0$. In keeping with the magnetic flux law, ϕ_1 must also be equal to zero for the surface supported by EFGHIJNME. From relation (7) it results that F_{od} must also be equal to 0. For the determination of the remaining parameters, the calculations necessary are similar to those performed for q-axis.

$$B_{g_{d1}} = \frac{4}{\pi}\int_o^{\pi/2} b_{g_{dr}}(\theta)\cos\theta \, d\theta \tag{19}$$

$$b_{g_{dr}} = -\mu_o \frac{\partial F(r,\theta)}{\partial r}\Big|_{r=R_5} ,$$

$$B_{g_{dc}} = B_{g_{B_{g_{d1}}}} . \cos\delta$$

$$K_{ad} = \frac{B_{g_{d1}}}{B_{g_{dc}}} , \tag{20}$$

$$\phi_d = \int_{-\pi/2}^{+\pi/2} b_{g_{dr}}(\theta).R_5 \, \ell.d\theta,$$

$$\phi_{d1} = \int_{-\pi/2}^{+\pi/2} B_{g_{d1}} \cos\theta. R_5.\ell \, d\theta,$$

$$\alpha_d = \frac{\phi_d}{\tau.\ell. B_{g_{dm}}} , \quad K\phi_d = \frac{\phi_d}{\phi_{d1}}$$

The integration of the Laplace equation in a polar coordinate system, over an area like the one in the previous case, is a difficult problem if done analytically. It requires the breaking down of the area into smaller ones and the subsequent summation of the solutions.

The digital approach is less laborious making possible the integration of the Laplace equation over the whole area at the same time.

3. COMPUTATION PROGRAM

For symmetry reasons, the digital integration is done only over half polar pitch. The integration domain, nodes and domain breakdown are presented in Fig.(3).

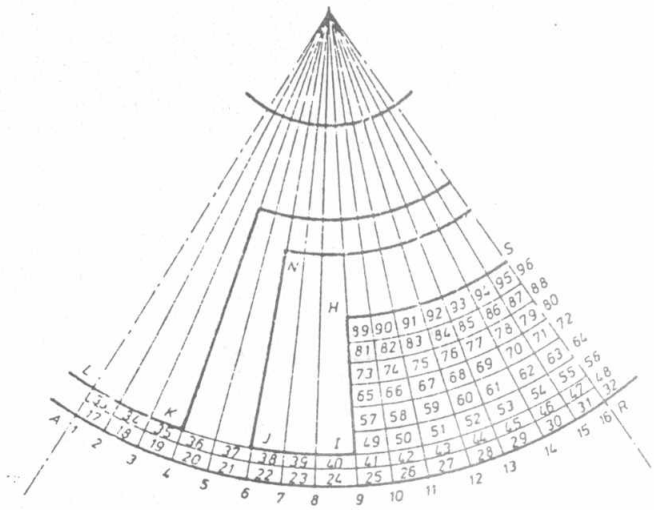

Fig.(3) Area used for the numerical integration

Finite differences were used for the integration techniques. The Laplace equation was modelled by a system of n equations with n unknown elements, which once it is solved, yield the scale magnetic potential for any node. The magnetizing force (the radial and tangential component) is obtained by derivation. In order to write the equations, $F(r,\theta)$ is expanded into Taylor power series around $i(r_i, \theta_i)$,

$$F_{i1} = F_i + r_{i1}\frac{\partial F_i}{\partial r_i} + \frac{r_{i1}^2}{2}\frac{\partial^2 F_i}{\partial r_i^2},$$

$$F_{i2} = F_i + \theta_{i2}\frac{\partial F_i}{\partial \theta_i} + \frac{\theta_{i2}^2}{2}\frac{\partial^2 F_i}{\partial \theta_i^2}, \qquad (21)$$

$$F_{i3} = F_i - r_{i3}\frac{\partial F_i}{\partial r_i} + \frac{r_{i3}^2}{2}\frac{\partial^2 F_i}{\partial r_i^2},$$

$$F_{i4} = F_i - \theta_{i4}\frac{\partial F_i}{\partial \theta_i} + \frac{\theta_{i4}^2}{2}\frac{\partial^2 F_i}{\partial \theta_i^2}$$

(for notations see Fig. (4))

The elimination of $(\partial^2 F_i/\partial r_i^2)$ and $(\partial^2 F_i/\partial \theta_i^2)$ from the first and third equation, from the second and fourth, respectively, yields :

$$\frac{\partial F_i}{\partial r_i} = \frac{r_{i3}^2 F_{i1} - r_{i1}^2 F_{i3}}{r_{i1} r_{i3}(r_{i1}+r_{i3})} + F_i \frac{r_{i1} - r_{i3}}{r_{i1} r_{i3}},$$

$$\frac{\partial F_i}{\partial \theta_i} = \frac{\theta_{i4}^2 F_{i2} - \theta_{i2}^2 F_{i4}}{\theta_{i2}\theta_{i4}(\theta_{i2} + \theta_{i4})} + F_i \frac{\theta_{i2} - \theta_{i4}}{\theta_{i2}\theta_{i4}} \qquad (22)$$

by using (21) and considering that for any i point the relation below is valid :

$$\frac{\partial^2 F_i}{\partial r_i^2} + \frac{1}{r_i}\frac{\partial F_i}{\partial r_i} + \frac{1}{\partial r_i^2}\frac{\partial^2 F_i}{\partial \theta_i^2} = 0,$$

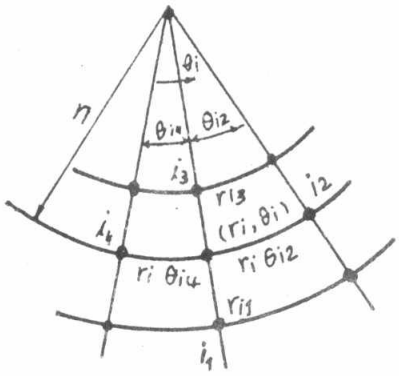

Fig.(4) Elementry integration area

One finds :

$$[2(\frac{1}{r_{i1}r_{i3}} + \frac{1}{r_i^2\theta_{i2}\theta_{i4}}) - \frac{1}{r_i}\frac{r_{i1}-r_{i3}}{r_{i1}\ r_{i3}}]-F_i - \frac{2r_i+r_{i3}}{r_i r_{i1}(r_{i1}+r_{i3})}F_{i1} -$$

$$\frac{2}{r_i^2\theta_{i2}(\theta_{i2}+\theta_{i4})}F_{i2} - \frac{2r_i+r_{i1}}{r_i.r_{i3}(r_{i4}+r_{i3})}F_{i3} - \frac{2}{r_i^2\theta_{i4}(\theta_{i2}+\theta_{i4})}F_{i4} = 0 \qquad (23)$$

which is equation i in the n system of equation, if i is an internal node for a boundary node :

$$F_i = F_{i\ boundary} \qquad (24)$$

4. RESULTS OBTAINED

By using a digital computer, the variation of coefficients K_{ad}, K_{aq}, α_q, $K\theta_d$, $K\theta_q$ is determined as a function of the rotor geometry and air-gap length, where the following used.

$\alpha_p = \frac{\theta_p}{\pi}$ - pole pitch covering coefficient;

$g = R_5 - R_4$ - air-gap length;

$h_p = R_4 - R_3$ - pole height ;

$h_{fe} = R_3 - R_2$ - yoke width ;

$h_{cn} = R_2 - R_1$ - non-magnetic channel width;

$\alpha_1 = 2\theta_a/\pi$

Fig.(6) shows that curves $K_{aq} = F(\alpha_1)$ have a minimum, the value α_1 reaches for this minimum varies with α_p. This is so because α_1 increases for α_p kept constant; and thus a decrease in the domain in which the air-gap field is reversed and as a result, K_{aq} rises. If α_1, decreases, MN increases and $\phi_1 = \phi_2 = \phi_q$ remain constant. F_o becomes smaller as shown by (7) also, the domain over which the air-gap field reverses decreases and consequently, K_{aq} will increase. The increase of K_{aq} with the pole height Fig.(7) seems surprising but it can be explained on the bases of relation (7). By varying h_p, $\phi_1 = \phi_2$ is kept increasing if the stator leakage flux

Fig.(5) Variation curves of coefficients K_{ad} and K_{aq} as a function of α_p, for different air-gap values.

For
$h_p/\tau = 0.2$, $\alpha_1 = 0.214$,
$h_{fe}/\tau = 0.066$, $h_{cn}/\tau = 0.714$,
$g/\tau = 0.0053$

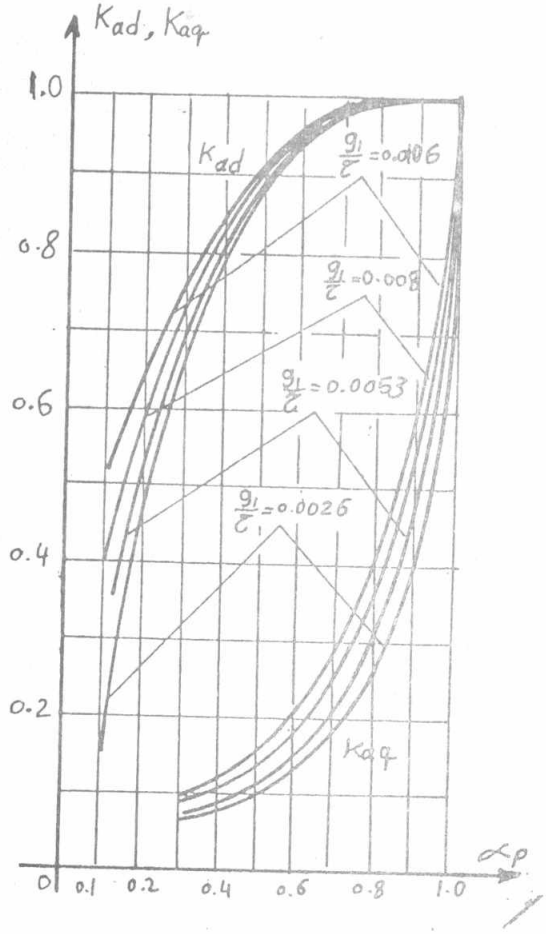

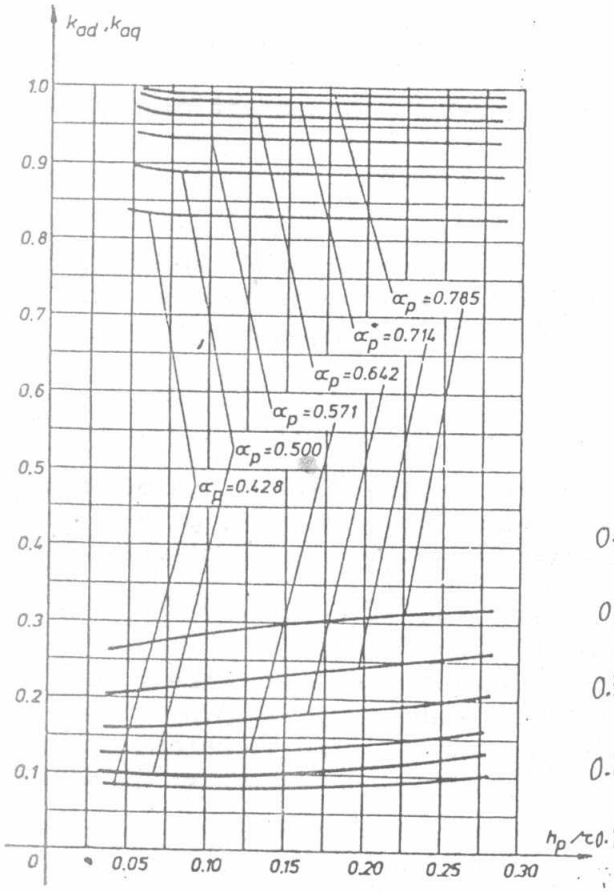

Fig.(7) Variation curves of coefficients K_{ad} and K_{aq} as a function of h_p/τ for different values of α_p.

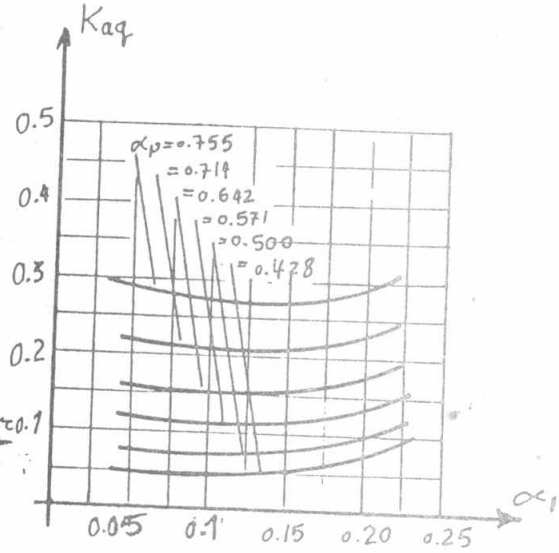

Fig.(6) Variation curves of coefficients K_{aq} as a function of α_1.

is neglected. By increasing h_p up to h_{fe} = const., JN rises and according to (7), F_o decreases and hence, K_{aq} increases. A maximum of the anisotropy coefficient, based on the results found so far, can be obtained for

$$\alpha_p = 0.5 \ , \ \alpha_1 = 0.1 \ , \ K_{ad} = 0.9 \ , \ K_{aq} = 0.075$$

$$K_{max} = (K_{ad}/K_{aq}) = (0.9/0.075) = 12.$$

For design purposes, the magnetic circuit must b taken into account, which is done by means of the saturation coefficient. Since for q-axis, the magnetic flux is rather low, the saturation coefficient (K_{sq}) is close to 1, while for d-axis, K_{sd} is 1.4 - 1.6.

The machine anisotropy real coefficient is lower, namely

$$K_r = \frac{K_{ad}}{K_{aq}} \cdot \frac{K_{sq}}{K_{sd}} = \frac{K}{K_{sd}} ,$$

which for this case can reach a maximum of

$$K_r = \frac{K}{K_{sd}} = \frac{12}{1.6} = 7.5$$

It follows that a non saturated machine will have a higher efficiency and power factors.

5. CONCLUSIONS

The determination of coefficients K_{ad} and K_{aq} is the most important part of the design of reluctance motors, as their ratio greatly influences the machine performances. The curves obtained allow the designers to make choice of the optimum rotor geometries.

REFERENCES

1] P.J.LAWRENSON, Developments in reluctance machine.Proceedings of EM 70 conference, University of Dundee, Scotland 1970, paper 39, p.39-4.

2] R.MAGUREANU,N.Vasile, Masini electerice speciale. Motorul sincron cu reluctanta variabila Bucuresti, I,P.B., 1979.

3] TR.MAGUREANU. The magnetic field and steady state parameters of flux reluctance motor Rev. Roum. p. 465-477, Tome 24-1979.

4] T.uguleu,C. Magnetic field, reactance and Torque of reactance synchronous machine Rev.-Roum. Sci. Tehn-Electrotehn.1965, 10,3,p.491-520.

5] R.MAGUREANU, N. Vasile. Calculul cimpului magnetic Si al parametrilor de regim stationar la motoral sincron Electrotechnica-Bucaresti 1979, 2, p. 54-58.